Immunity 24, 429–438, April 2006 ©2006 Elsevier Inc. DOI 10.1016/j.immuni.2006.02.010

# Differential Epitope Positioning within the Germline Antibody Paratope Enhances Promiscuity in the Primary Immune Response

Dhruv K. Sethi,[1] Anupriya Agarwal,[1] Venkatasamy Manivel,[2] Kanury V.S. Rao,[2] and Dinakar M. Salunke[1,*]
[1] National Institute of Immunology
New Delhi 110067
India
[2] International Center for Genetic Engineering and Biotechnology
New Delhi 110067
India

## Summary

**Correlation between the promiscuity of the primary antibody response and conformational flexibility in a germline antibody was addressed by using germline antibody 36-65. Crystallographic analyses of the 36-65 Fab with three independent dodecapeptides provided mechanistic insights into the generation of antibody diversity. While four antigen-free Fab molecules provided a quantitative description of the conformational repertoire of the antibody CDRs, three Fab molecules bound to structurally diverse peptide epitopes exhibited a common paratope conformation. Each peptide revealed spatially different footprints within the antigen-combining site. However, a conformation-specific lock involving two shared residues, which were also associated with hapten binding, was discernible. Unlike the hapten, the peptides interacted with residues that undergo somatic mutations, suggesting a possible mechanism for excluding "nonspecific" antigens during affinity maturation. The observed multiple binding modes of diverse epitopes within a common paratope conformation of a germline antibody reveal a simple, yet elegant, mechanism for expanding the primary antibody repertoire.**

## Introduction

Antigen recognition and subsequent affinity maturation fundamentally interface physical principles of molecular interactions with the physiological processes associated with self-nonself discrimination. Although a large body of crystallographic data generated over the past two decades has facilitated understanding of the structural basis of immune recognition itself, data with regard to the primary antibody response have been limited (Wedemayer et al., 1997; Yin et al., 2001, 2003; Romesberg et al., 1998; Nguyen et al., 2003). As a result, the portrait of the downstream processes that lead to evolution of antibody affinity after the initial encounter of the B cell receptor with the antigen is fuzzy.

The naive primary immune repertoire involves a vast array of B lymphocytes possessing germline antibody receptors. This repertoire can respond to any incoming antigen without having been previously exposed to it. Recognition of the incoming antigen requires the generation of a vast array of unique specificities in the naive repertoire. Explanations for the diversity of the antibody repertoire have mostly explored genetic recombination processes in germline gene segments (Tonegawa, 1983). Enigmatically, however, the numbers of functionally active antibody genes generated in an individual, and the B lymphocytes that bear them, are far too few when compared with the range of potential antigens encountered (Cook and Tomlinson, 1995). Therefore, additional mechanisms are likely to exist to recognize the practically infinite antigenic distribution by using a limited antibody repertoire.

Logically, such mechanisms would require a given germline antigen receptor to engage multiple antigens. Indeed, utilization of wider conformational space for generating diverse specificities has been proposed as a possible mechanism and is supported by thermodynamic data (Manivel et al., 2000). In other words, the intrinsic conformational flexibility of the germline antibody was suggested to facilitate its binding to multiple antigens. A similar structural plasticity for the combining site of the T cell receptor (TCR), governing its interaction with the cognate peptide-MHC complex, has also been suggested (Garcia et al., 1998). However, while the existence of flexible antigen-combining sites has been widely recognized, the role of conformational flexibility in the adaptive immune system has not yet been structurally elucidated. Whether such a property would eventually prove beneficial to immune function will largely depend on the degree of flexibility inherent to the antigen-combining site (paratope). It was with the intent of quantitatively analyzing this issue and deciphering the correlation of the flexibility of the paratope on one hand, and the pluripotency of the initial antibody response on the other, that the present study was undertaken.

We have structurally investigated how a germline antibody can bind a diverse set of antigens and analyzed the implications of this crossreactivity. The system used for these studies was a germline monoclonal antibody, 36-65, which was initially identified in the context of an immune response against the hapten p-azophenylarsonate (Ars). The antibody has been used extensively for addressing specificity and affinity in the antibody response (Strong et al., 1991; Parhami-Seren et al., 1993; Vora et al., 1998; Robertson et al., 1982). Mature antibody 36-71 against Ars is derived from germline antibody 36-65 through somatic hypermutation, accumulating 19 changes during the process of affinity maturation (Sharon et al., 1989). Antibody 36-65 has an affinity for the hapten (Ars) of 8.1 $\mu$M ($K_d$), which showed a 40-fold decrease when the temperature was increased from 25°C to 35°C, implying the existence of conformational flexibility in the germline antibody. In contrast, the corresponding mature antibody 36-71 had an affinity of 0.06 $\mu$M ($K_d$) for the hapten, which upon increasing the temperature to 35°C, changed only marginally, effectively indicating relative rigidity in the affinity-matured antibody (Manivel et al., 2000).

*Correspondence: dinakar@nii.res.in

Table 1. Binding Affinities and Amino Acid Sequences of the Dodecapeptides Derived from a Phage-Displayed Random Peptide Library against Germline Antibody 36-65

| Clone Number | Peptide Sequence | $K_d$ (μM) |
|---|---|---|
| 65-37.18 (RII) | RLLIADPPSPRE | 0.15 |
| 65-37.28 (KIa) | KLASIPTHTSPL | 0.12 |
| 65-04.04 (SIg) | SLGDNLTNHNLR | 0.21 |

Data are taken from Manivel et al. (2002).

The recognition of a variety of unrelated antigens by a germline antibody and its implications for the generation of diversity in the primary antibody response and subsequent affinity maturation were subjected to crystallographic investigations. A series of independent peptides, which bind to germline antibody 36-65 with affinities comparable to that of Ars, was selected by screening a 12-mer phage-displayed random peptide library (Manivel et al., 2002). Crystallographic studies involving germline antibody 36-65 in the antigen-free form and in complex with three distinct dodecapeptides reported here provide direct molecular images corresponding to the conformational variability extant in an individual germline antibody. However, contrary to expectations, a single conformational state of the paratope was alone found to be capable of recognizing these diverse independent dodecapeptides. The observed variety in the modes of epitope juxtaposition while interacting with the paratope indicates the generation of antibody diversity, even within a single conformational state.

## Results

Cocrystallization of the 36-65 germline antibody Fab with unrelated synthetic dodecapeptides was attempted in order to obtain high-resolution images of the germline antibody Fab-peptide complexes and to compare them with those of the antigen-free germline antibody. After exploring nine independent peptides of relatively high affinity, we succeeded in obtaining diffraction-quality crystals for three 36-65 Fab-peptide complexes (Table 1) in addition to the crystals of the antigen-free germline 36-65 Fab.

### The Database

Crystal data and refinement statistics for all four of the structures are shown in Table 2. The structure of each of the Fab molecules has four standard immunoglobulin folds, two each for the heavy and the light chains, respectively. All of the complementarity-determining regions (CDRs) and disulfide bridges were clearly visible in the electron density and could be reliably deciphered. Molecular replacement for the unliganded germline antibody Fab was carried out by using the structure of affinity-matured antibody 36-71 (Strong et al., 1991). The two molecules in the asymmetric unit of the native antibody (Nat-Fab) were named Nat-AB and Nat-LH. Ribbon drawings describing the structures of the two Fab molecules of Nat-Fab are shown in Figure 1. Structural properties of the two independent Fab molecules quantified in terms of elbow angles and $V_H$-$V_L$ interfaces for this structure as well as the other structures are listed in Table S1 (see the Supplemental Data available with this article online).

The structure of the complex of peptide KIa with Fab (KIa-AB), determined at 2.5 Å resolution, is shown in Figure 1. The asymmetric unit contained a single molecule of the complex. Nine residues of the peptide, Ser4–Leu12, with unit occupancy were evident in the electron density. The RII-Fab complex had two molecules, RII-LH

Table 2. Crystallographic Parameters of the Four Crystal Structures Involving a Germline Antibody 36-65 Fab Fragment

| Parameter | Antigen-free | KIa | RII | SIg |
|---|---|---|---|---|
| Space group | $P2_1$ | $P2_1$ | $P2_1$ | $P2_1$ |
| Cell constants (Å) | | | | |
| a | 75.0 | 54.2 | 53.3 | 53.1 |
| b | 73.7 | 77.0 | 145.8 | 144.9 |
| c | 85.8 | 59.1 | 71.3 | 71.0 |
| β | 113.9° | 102.0° | 104.4° | 104.3° |
| Maximum resolution (Å) | 2.7 | 2.5 | 2.9 | 3.0 |
| Resolution range (last shell Å) | 2.8–2.7 | 2.59–2.5 | 3.0–2.9 | 3.11–3.0 |
| Completeness (%) | 85.3 (86.7)[a] | 94.2 (96.3) | 83.0 (82.1) | 94.9 (95.9) |
| Number of observed reflections | 60,734 | 45,923 | 97,679 | 60,062 |
| Number of unique reflections | 23,857 | 15,724 | 23,421 | 19,662 |
| Multiplicity | 2.54 | 2.9 | 4.17 | 3.04 |
| Average(I)/(σI) | 6.91 (1.9) | 5.1 (1.7) | 6.87 (2.2) | 4.0 (1.4) |
| $R_{merge}$ (%) | 9.5 (31.9) | 10.4 (31.3) | 13.0 (41.4) | 12.0 (32.3) |
| Number of solvent atoms | 137 | 55 | 78 | 103 |
| $R_{cryst}$ (%) | 22.5 | 24.5 | 23.0 | 24.5 |
| $R_{free}$ (%) | 26.5 | 26.4 | 26.4 | 26.4 |
| B factors (protein) | 18.4 | 21.0 | 23.6 | 34.0 |
| B factors (peptide) | — | 55.5 | 64.8 | 50.0 |
| Rms deviation (bond length) | 0.013 | 0.008 | 0.012 | 0.010 |
| Rms deviation (bond angle) | 1.79 | 1.68 | 1.83 | 1.73 |
| Ramachandran plot | | | | |
| Allowed regions (%) | 96.5 | 97.4 | 96.9 | 96.6 |
| Generously allowed region (%) | 2.3 | 1.6 | 2.1 | 2.3 |
| Disallowed region (%) | 1.2 | 1.1 | 0.9 | 1.1 |

[a] Numbers in parentheses correspond to the highest-resolution shell.

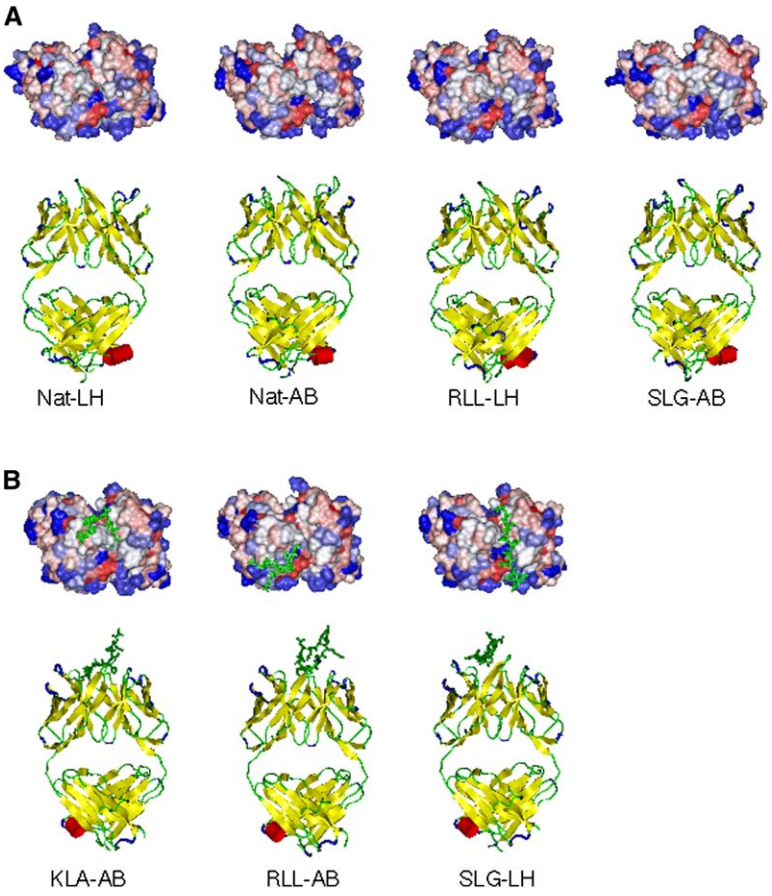


Figure 1. Seven Crystallographically Independent Molecules of the 36-65 Germline Antibody Fab

(A) The four antigen-free states of the antibody are shown in a ribbon drawing, highlighting the secondary structure. The CDRs of the corresponding molecules represented as Connolly surfaces are decorated according to hydropathy features (red, hydrophobic; blue, charged) and are shown in a view perpendicular to that of the ribbon drawing.

(B) The three peptide bound states shown in the ribbon drawing, highlighting secondary structural features. CDRs of the corresponding molecules represented as Connolly surfaces are decorated according to hydropathy features (red, hydrophobic; blue, charged) and are shown in a view perpendicular to that of the ribbon drawing. Peptide molecules in each case are shown as green sticks.

(Figure 1A) and RII-AB (Figure 1B), in the asymmetric unit. While RII-AB showed electron density corresponding to the entire peptide with an occupancy of 0.8, RII-LH did not show any significant electron density corresponding to the peptide at the antigen-combining site (Figure S1). The structure of the Slg-Fab complex also revealed two molecules, Slg-LH (Figure 1B) and Slg-AB (Figure 1A), in the asymmetric unit. Electron density for 10 residues of the peptide (occupancy of 0.7) bound to Slg-LH was evident. However, no electron density for the peptide was observed in the case of Slg-AB. Additionally, the molecular packing in both RII-LH and Slg-AB was such that adequate space was not available for accommodating the peptide within the antigen-combining site. The electron density maps of the peptides observed in the structures of the three Fab-peptide complexes, Kla-Fab, RII-Fab, and Slg-Fab, are shown as stereoscopic images in Figure S2. In all three Fab-peptide complexes, the electron density for the heavy chain loop Ser136H–Asn141H was ambiguous, as in many other reported antibody Fab structures (Young et al., 1997). Comparisons of the CDR conformations of the two Fab molecules in the asymmetric units of each of the crystal structures, Nat-Fab, RII-Fab, and Slg-Fab, showed differences to varied extents in each structure (Figure S3).

Thus, a database of seven Fab molecules (Figure 1) was available from the four crystal structures determined. These included the three antigen bound Fab molecules, Kla-AB, RII-AB, and Slg-LH, in which bound peptide had been identified and the four antigen-free molecules, Nat-AB, Nat-LH, RII-LH, and Slg-AB. The Fab molecules Nat-AB and Nat-LH are from the Fab crystallized in the absence of the antigen, while the remaining two were from the crystal structures of the RII-Fab complex (RII-LH) and the Slg-Fab complex (Slg-AB). The high sensitivity of the germline antibody affinity to environmental perturbations (Manivel et al., 2000) may have been responsible for some loss in antigen-antibody affinity under the crystallization conditions. Lower effective affinity combined with the steric constraints in the antigen-combining site could have facilitated absence of the peptide (as evident from the electron density map) in one of the two molecules in the asymmetric unit, enabling us to consider RII-LH and Slg-AB as antigen-free states.

### Antigen-free Germline Antibody Structures

Analysis of the four antigen-free Fab molecules from three crystal structures revealed the structural diversity associated with the germline antibody (Figure 1). The elbow angles of the four molecules show a range of 7.5°, varying from 171.3° to 178.8° (Table S1). Analysis of the $V_H$-$V_L$ interface in terms of buried surface area, one of the parameters determining diversity in binding abilities, was found to exhibit a much larger distribution for the antigen-free structures (1528–1768 Å$^2$) compared to the antigen bound structures (1558–1656 Å$^2$).

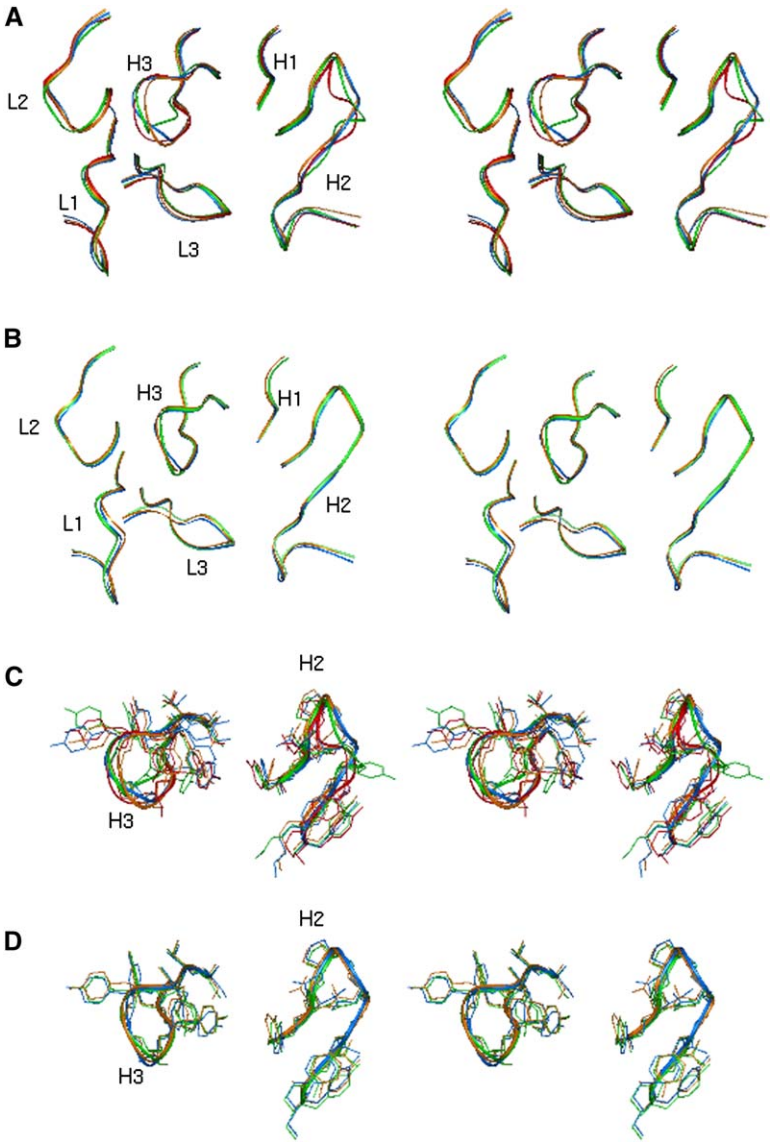


Figure 2. Stereoscopic Representation of CDR Loop Conformations of the Antigen-free and Antigen Bound Fab Molecules of Antibody 36-65

(A) Superimposition of CDR regions of four antigen-free Fab molecules represented as thin ribbons. The color codes are: red, Nat-AB; green, Nat-LH; blue, Slg-AB; orange, RII-LH.

(B) Superimposition of CDR regions of the three antigen bound Fab molecules shown as thin ribbons. The color codes are: blue, Slg-LH; green, Kla-AB; orange, RII-AB.

(C and D) The CDRs H2 and H3 of (C) antigen-free and (D) antigen bound molecules corresponding to (A) and (B), respectively, are highlighted with backbone as well as side chain conformations superimposed.

The surface features of the CDRs of the four Fab molecules decorated with hydropathy features are shown in Figure 1A. No two molecules exhibit similar topologies; differences are apparent in the charge distribution and the hydropathy features. Both backbone conformations and side chain orientations contribute to these differences. Topological differences could be correlated with differences in the backbone conformations, which were evident upon the superimposition of the $C_\alpha$ atoms of each of these molecules (Figure 2A). It was found that the conformations of CDR loops H2 and H3 were substantially different in each of the antigen-free molecules. Upon superimposition of the CDRs of the two independent molecules, Nat-AB and Nat-LH, a maximum $C_\alpha$ distance of 3.4 and 2.4 Å was observed between the corresponding $C_\alpha$ atoms of CDRs H2 and H3, respectively (Figure S4A). The $C_\alpha$ rmsds over the entire loops were 1.2 and 1.0 Å for H2 and H3, respectively. The backbone and side chain conformational variations observed in CDRs H2 and H3 are shown in Figure 2C.

## Peptide Antigen Bound Germline Antibody Structures

As the CDRs in the germline structures were found to exist in multiple conformations, we sought to investigate if this conformational diversity was indeed exploited while binding to disparate antigens. Surprisingly, the surface analysis of the Fab molecules in the bound form indicated similarity of their paratope topologies (Figure 1B). This similarity was even more perceptible from the $C_\alpha$ superimposition (Figure 2B), with CDRs H2 and H3 showing an excellent overlap in the three antigen bound structures (Figures 2B and 2D). The rmsds of $C_\alpha$ atoms on pairwise CDR superimpositions were found to be consistently below 0.3 Å for H2 and less than 0.5 Å for H3. The maximum $C_\alpha$ distance for corresponding residues also did not exceed 0.9 Å in any of the pairs (Figure S4A). Thermal parameters (B factors) were analyzed for all seven molecules. The B factors for CDRs H2 and H3 of peptide bound molecules were significantly lower than those for the antigen-free molecules. This is evident from the comparison of the B factors for the antigen

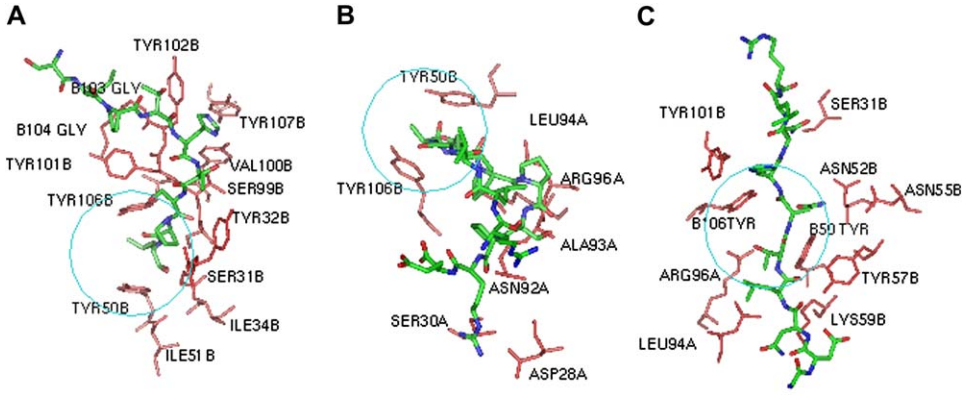


Figure 3. Residues of Germline Antibody 36-65 Involved in Peptide Binding

(A–C) Interactions of the peptides (A) Kla, (B) RII, and (C) Slg with the Fab in corresponding crystal structures. Residues of the Fab molecules (within 4 Å of the bound peptide) are shown as red sticks, and the peptides are shown as sticks in elemental colors. The only common interacting residues, Tyr50 and Tyr106, among the three complex structures are highlighted with a circle.

bound and antigen-free Fab molecules in the crystal structures of RII-Fab (Figure S4B) and Slg-Fab (Figure S4C).

A comparison of the mode of binding of the three peptide antigens to antibody 36-65, highlighting the residues involved in the interaction, is shown in Figure 3. All three of the peptides were seen bound to independent residues on spatially different sections of the CDRs in entirely unrelated conformations (Figure 1B). Although the thermal parameters of the peptides are relatively higher than those of the CDRs of corresponding Fab molecules (Table 2; Figure S4), the interactions were specific, as many hydrogen bonding and salt bridge contacts were observed (Table S2).

Although all three peptides exhibited contacts with CDRs H3 and H2, as well as with the light chain CDRs, the degree of involvement differed. Broadly, while Kla wound around CDRH3 in a loop-like conformation, contacting residues Ser99H, Tyr101H, Tyr102H, Gly103H, Gly104H, and Tyr106H, the peptide, Slg, which lies in an extended conformation positioned at the interface of the variable heavy and light chain domains of the Fab, showed major interactions with CDRH2 and mainly contacted Asn52H, Asn55H, Tyr57H, and Lys59H. In contrast with the primarily heavy chain contacts of the other two peptides, RII, which resembles a hairpin, folded through the middle at Asp6, predominantly interacted with CDRL3 of the antibody; this interaction involved residues Asn92L, Thr93L, Leu94L, and Arg96L. Additionally, several hydrophobic residues of RII are involved in intrapeptide interactions, rendering them relatively solvent inaccessible. In all, 26 residues of the Fab CDRs were involved in interacting with the peptides in one case or the other. However, only 2 among these 26 residues, Tyr50H and Tyr106H, were common among the 3 Fab-peptide complexes, underscoring the distinct modes of binding (Table S2).

### Comparison between Antibody Binding by the Hapten p-Azophenylarsonate and the Peptide Antigens

The binding modes of the three peptides with germline antibody 36-65 were analyzed in the context of that of the hapten, Ars, with the corresponding affinity-matured antibody 36-71 (Strong et al., 1991). A model of 36-71 Fab bound to Ars built on the basis of a low-resolution electron density map of the complex of Ars with 36-71 Fab and biochemical data (Parhami-Seren et al., 1993; Sompuram and Sharon, 1993; Strong et al., 1991) was used for this purpose. In spite of binding at different spatial locations in independent modes, each one of the peptides managed to interleave at least 1 residue within the Ars binding site, critically flanked by residues Tyr50H and Tyr106H (Figure 3). Comparisons of the side chain conformations of residues in the vicinity of the Ars binding site in the four antigen-free germline antibody Fab molecules showed that they had significant differences with each other as well as with corresponding residues of affinity-matured antibody 36-71 (Figure 4B). On the other hand, the antigen bound antibodies showed better superimposition, in favor of the conformation of the affinity-matured antibody (Figure 4C).

We analyzed the nature of antibody-peptide binding in the present study in light of the known Fab-peptide crystal structures. The buried interfacial areas upon binding, 958, 633, and 720 $Å^2$ in the case of Kla-AB, RII-AB, and Slg-LH, respectively, were similar to those in other peptide-antibody complexes (Wilson and Stanfield, 1993; Webster et al., 1994). The buried surface area contributions of the heavy chain in Kla-AB and Slg-LH were more than 80%, while that of RII-AB was about 25%. Although antigen binding predominantly involves the heavy chain, exceptions showing major contributions from the light chain do exist (Nair et al., 2000). Interactions of 20 independent antibodies bound to their corresponding peptide antigens, highlighting the footprints of their interactions, were compared with the corresponding footprints in germline antibody 36-65 (Figure 5). It was evident from the comparison that the Fab molecules generally use a subset of residues for binding to independent peptides from the larger pool of residues that define the CDRs. Although most of the peptides primarily interact with residues from CDRH3, those from other regions were also involved. Diverse regions were buried by different antigenic peptides while binding to their corresponding antibodies.

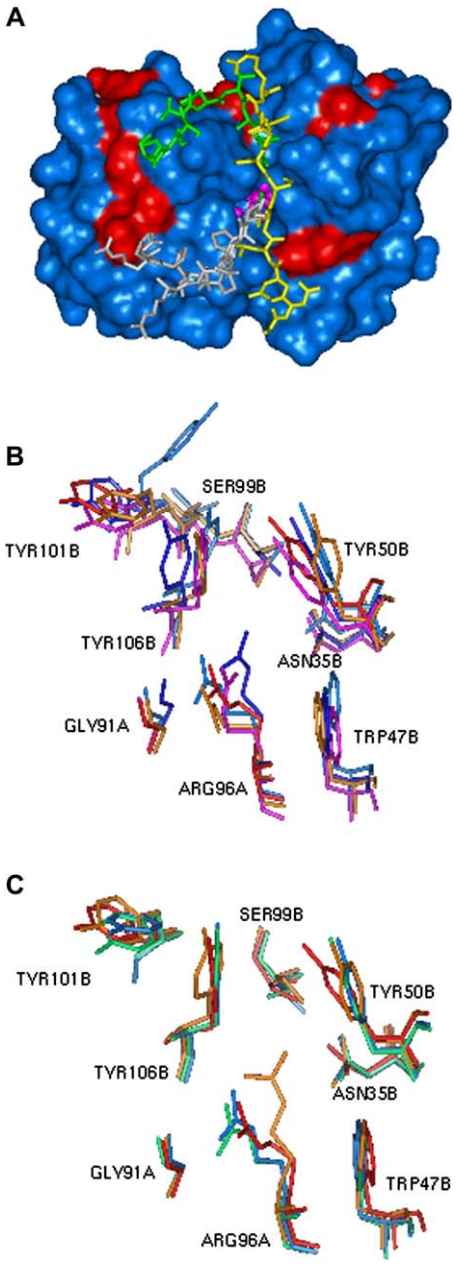


Figure 4. Structural Properties of the Interacting Surface of the 36-65 Fab in the Context of Antigen Binding

(A) Superimposition of the three peptides bound to germline antibody 36-65 onto the surface of affinity-matured antibody 36-71; residues that mutate during affinity maturation are shown in red. The hapten, Ars, is shown in magenta as balls and sticks.

(B and C) Superimposition of the residues within a 5 Å radius of the arsonate binding site in (B) antigen-free structures and (C) antigen bound structures.

## Discussion

Degenerate recognition specificity of the primary antibody response has been a focus of attention in the context of affinity maturation in T-dependent humoral immune responses (Manivel et al., 2000; Yin et al., 2003). The seven Fab molecules of germline antibody 36-65 in different crystallographic environments described here provide valuable insights into the generation of diversity and the antigen-driven education of the primary antibody response during affinity maturation. While antigen-free molecular structures of 36-65 Fab provided a quantitative description of the conformational repertoire of the CDRs, the peptide antigen bound structures facilitated deciphering of the structural intricacies of degenerate specificity associated with germline antibodies.

### Observed Conformational Flexibility in Antigen-free Germline Antibody 36-65 Is Not Utilized while Recognizing Multiple Independent Antigens

While conformational isomerism was observed in mature antibodies during antigen binding (Foote and Milstein, 1994), germline antibodies were suggested to be even more flexible (Manivel et al., 2000). In the case of germline antibody 36-65, we have been able to structurally image the anticipated conformational variability of CDRs in the absence of antigen. Variability was evident in terms of elbow angles, $V_H$-$V_L$ interfaces, as well as the surface features. The wide conformational heterogeneity observed in the four independent molecular structures of the same germline antibody Fab illustrates the extent of structural diversity in a typical germline antibody paratope. Indeed, the two molecules (Nat-AB and Nat-LH) in the Fab crystals obtained in the absence of any antigen show the largest conformational variation amongst the antigen-free Fab molecules and establish the range of variability that exists in the antigen-combining site of germline antibody 36-65.

Having confirmed the conformational heterogeneity in the germline antibody CDRs, we next sought to elucidate its correlation with polyspecificity. Although polyspecificity has been observed in affinity-matured antibodies (Foote and Milstein, 1994, Keitel et al., 1997, James et al., 2003), it is anticipated to an even greater extent in germline antibodies. Direct correlation of conformational flexibility and polyspecificity has been proposed in germline antibodies (Wedemayer et al., 1997; Manivel et al., 2002). The affinity-matured antibodies SPE7 (James et al., 2003) and 2D10 (Goel et al., 2004), both of which bind varied antigens, have been shown to adopt multiple conformational states in equilibrium. In affinity-matured antibodies, conformational flexibility may be the cause and polyspecificity may be the effect. In contrast, germline antibodies show pluripotency as a physiological prerequisite and are expected to possess the ability to bind diverse antigens as part of the pristine antibody response.

Exploitation of the observed flexibility in germline antibody structures to bind diverse antigens could be addressed by simply comparing the mode of binding of germline antibody 36-65 with three independent peptide antigens. Surprisingly, CDRs of the three peptide bound Fab molecules, which were conformationally divergent in the antigen-free Fab structures, showed an excellent overlap in terms of both side chain and backbone conformations. Thus, while the germline antibody exhibited conformational heterogeneity in the absence of any antigen, it exists in a common conformation in all three of the peptide bound structures.

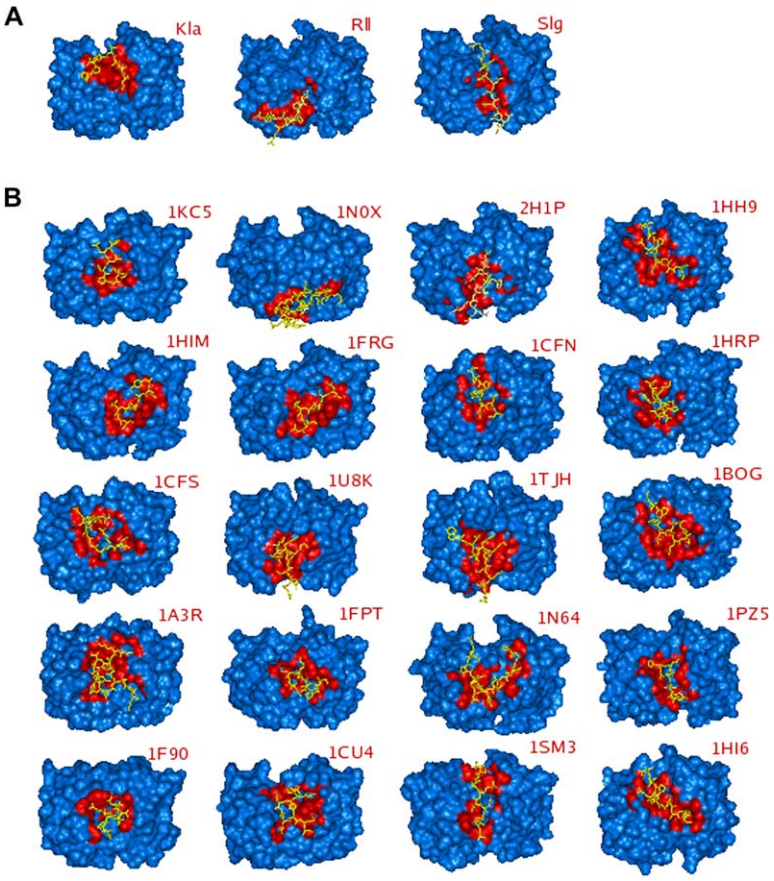


Figure 5. Comparison of the Footprints of Phage Display-Derived Peptides on Germline Antibody 36-65 with Other Peptide-Antibody Complexes Derived from the PDB

(A) The three dodecapeptides, Kla, RII, and Slg, bound to germline antibody 36-65.

(B) The binding of 20 different peptide antigens to their corresponding antibodies. The structures are identified by their PDB codes. The paratope of the antibody molecule is shown as Connolly surfaces (blue), and the surface area buried upon peptide binding is highlighted (red).

### Conformational Congruence while Binding to Diverse Antigens of the Otherwise Flexible Germline Paratope May Be Linked to the Evolution of Specificity

It was pertinent to address why a common structure should be adopted upon binding, particularly since the potential for structure modulation was found to be intrinsic to germline antibody 36-65. Any possibility that the common paratope conformation could be achieved through molecular mimicry in epitope-paratope interactions would be viable only if structural similarity in epitopes leads to similar modes of interaction with the paratope. While the three structurally independent peptides utilized vastly different spatial distributions on the antibody paratope for binding to the germline antibody, interactions with two residues of the antibody, Tyr50H and Tyr106H, were conserved among all three of the Fab-peptide complexes. Incidentally, these residues have also been suggested to be critical for binding of the hapten, Ars, to affinity-matured antibody 36-71 (Sompuram and Sharon, 1993). However, the modes of binding of the four antigens, including Ars, to these two tyrosines were very different. Whereas Ars bound through the stabilization of $\pi$-$\pi$ interactions sandwiching the phenyl ring between Tyr50H and Tyr106H, Kla inserted a hydrophobic residue, Leu12, between them. An acidic residue, Asp6, was involved in RII, and Slg utilized the peptide backbone for binding. Hence, the three peptides did not show any structural similarity, nor was there any correlation found in the epitope-paratope interactions involving them.

Thus, while the broad recognition potential of the germline antibody was evident, an epitope interaction involving contacts with only two shared residues of the paratope seems to be adequate for maintaining the stability of a given conformational state. In that sense, the two common tyrosine residues may define a conformation-specific "lock" in the germline antibody, which favors a particular conformational state for the CDRs. It is not essential that every unrelated antigen binding to the germline antibody will be involved in activating the "critical" residues, which lock a particular conformation. Binding of porphyrin and jeffamine to a germline antibody (Yin et al., 2003) showed two distinct conformational states, implying that jeffamine does not bind to the critical set of residues that may correspond to the porphyrin-specific paratope conformation. It has been suggested that primary germline antibodies bind to a given antigen through one of many preexisting isomers. In fact, the canonical conformations that have been characterized in affinity-matured antibody repertoires against diverse antigens (Chothia and Lesk, 1987; Chothia et al., 1989) may correspond to some of these preexisting conformational states in the germline.

Analysis of antibodies of known structures suggests a lack of correspondence between the residues in contact with the antigen and those modified by somatic mutations. This is explained in terms of mutations in contacting residues having an adverse effect on the antigen-antibody interactions (Ramirez-Benitez and Almagro, 2001). Indeed, the residues of germline antibody 36-65 that undergo mutations leading to mature antibody

36-71 are considerably distant from the Ars binding site. While the three peptides used here bound to antibody 36-65 with comparable affinities, none of them was recognized by affinity-matured antibody 36-71 (Manivel et al., 2002). Analysis of the interactions of the paratope with the peptide antigens may provide an explanation for this observation. Some of the residues of the germline antibody that undergo somatic mutations in the process of evolving higher affinity toward Ars are seen to be involved in peptide binding. Elimination of these interactions during affinity maturation might explain exclusion of binding of the peptides in an antibody matured to be specific for Ars (Figure 4A), providing an elegant mechanism of excluding otherwise "nonspecific" antigens during affinity maturation.

Recognition of diverse antigens by a single paratope structure would only be possible by compromising on the stringency in the nature of interactions otherwise associated with specific recognition. The relatively pliable initial encounter of the antigen in the primary antibody response may, in fact, facilitate such pluripotency. The persistence of antigen during affinity maturation of antibodies (Wang et al., 2000) would enable the continuing interaction of the antigen with conformation-specific residues, such as Tyr50H and Tyr106H in the present case, to suitably lock the structural state for antigen recognition. This structural state would then be further stabilized through somatic mutations during affinity maturation. Thus, the conformation-specific interactions built in within the antigen-combining site may well be utilized for modulating antibody specificity during affinity maturation.

### Juxtapositional Variety in Epitope-Paratope Interaction Is Involved in the Generation of Diversity in the Primary Antibody Response

Distribution of the three dodecapeptides over the paratope surface indicated widespread utilization of the antigen-combining region. Each one of the peptide antigens binds to a different part of the paratope, defining a footprint of that antigen, while the CDR conformations remain identical in each case. This ability of the antibody, wherein multiple antigens can be recognized through differential juxtapositioning, has implications for the generation of diversity. Interestingly, the footprints of the dodecapeptide epitopes on germline antibody 36-65 resembled those of other independent peptide antigens when bound to their corresponding antibodies. A comparison of 20 independent affinity-matured antibodies bound to their corresponding peptide antigens showed that the antibody molecules generally use a subsite from within the larger combining region for binding to independent antigens. Each one of these affinity-matured antibodies would have arisen from germline precursors in which the initial peptide binding would have taken place in the conformation and the spatial location finally observed in the affinity-matured antibody. Apparently, the entire antigen-combining region is equipped with a propensity for interaction. Taking into account the spatial distribution of the bound peptides on the mature antibody paratope and the likely ability of the precursor germline antibody to use the entire antigen binding region, it can be extrapolated that germline antibodies commonly utilize alternative juxtapositions for enhancing binding ability.

Although genetic recombinations principally account for antibody and TCR diversity, the immune response is still limited by the number of possible unique combinations and circulating lymphocytes. Crossreactivity is thus a necessary requirement to overcome bottlenecks in a rapid immune response due to limiting frequencies of particular specificities (Mason, 1998). Crossreactivity as a solution to this discrepancy between the limited germline repertoire and the vast antigenic space was believed to arise from the conformational flexibility of the antibody (Manivel et al., 2002). However, our analysis has illustrated that within a given conformational state of the antigen-combining site, diverse modes of antigen recognition are possible, suggesting yet another way of generating diversity. This is also consistent with the suggestion that the B cell receptors in the primary repertoire possess a bipartite binding site in which CDR H3 acts as an antigen-specific core, whereas other CDRs contribute in an opportunistic fashion (Davis, 2004). In a broader context, diversity in enzymatic reactions through similar active site conformations is more common than the promiscuity mediated by conformational diversity (James and Tawfik, 2003). Similarly, in epitope-paratope interactions, independent antibodies prefer a common conformation while binding to a flexible antigen even if they assume different structures in the absence of the antigen (Nair et al., 2002). Multifunctionality without involving conformational flexibility may actually be preferred since the generation of diverse structures from the same sequence would involve complex folding issues.

To summarize, while four antigen-free Fab structures quantitatively defined the conformational repertoire of the CDRs, analysis of the antigen bound Fab structures offered mechanistic insights into the generation of antibody diversity. Although the flexibility in the CDRs was structurally apparent, it was striking that a single paratope conformation recognized multiple independent epitopes such that the binding of dissimilar antigens represented autonomous epitope footprints on the antibody-combining site. The two common antibody residues may actually define a conformation-specific lock associated with one among multiple conformational states of the germline antibody. Thus, the observed multiple binding modes of independent epitopes within a single paratope conformational state reveal, to the best of our knowledge, a novel mechanism—wherein variety in the paratope-epitope juxtaposition was exploited—for expanding the germline antibody repertoire.

## Experimental Procedures

### Peptides

Several independent peptides selected from a panel of phage-displayed peptides shown to bind to the germline antibody (Manivel et al., 2002) were used for cocrystallization experiments. Reasonably high affinity for germline antibody 36-65 and excellent aqueous solubility were the two criteria used for selecting the peptides from the panel. The 12-mer peptides were synthesized by the solid-phase method on an automated peptide synthesizer (431A; Applied Biosystems, Foster City, CA). Cleavage was performed by using trifluoroacetic acid (Sigma-Aldrich). Crude peptides were purified on a Delta Pak C18 column (Waters, Milford, MA) by using a linear

gradient of acetonitrile containing 0.1% trifluoroacetic acid. The peptides were characterized by mass spectroscopy.

### Antibody

Hybridoma cells secreting IgG 36-65 and suspended in 500 μl Dulbecco's phosphate-buffered saline (DPBS) were injected into the peritoneal cavity of male BALB/c mice γ irradiated (400 rads) and primed with Freund's incomplete adjuvant 72 hr prior to injecting the hybridoma cells. A total of $5 \times 10^5$ to $5 \times 10^6$ hybridoma cells were injected into each mouse. Ascitic fluid could be tapped from the peritoneal cavity of mice after ~4–5 days. The animal experiments were approved by the Institutional Animal Ethics Committee.

### Fab Preparation

The IgG was purified from mouse ascitic fluid. A 40% ammonium sulfate precipitation was followed by resuspension of the precipitate in 10 mM Tris (pH 8.5). Further purification of the IgG was carried out by ion exchange chromatography by using a DEAE 5PW anion exchange column. Fab fragments of the antibody were prepared by papain digestion of the purified IgG at pH 7.1, and the Fab was purified from the digestion mix by using DEAE anion exchange chromatography. The purity was checked by SDS-PAGE, and the concentration of the Fab was estimated by protein assay (Bio-Rad, Hercules, CA) by using BSA as the standard.

### Crystallization

Initial crystallization trials for the native Fab crystals involved the exploration of various precipitants, typically metal salts in combination with polyethylene glycols of various molecular weights. Combinations of $ZnCl_2$ with polyethylene glycol (8.0 kDa) initially gave reasonable crystals that diffracted to a resolution of 3.0 Å or better. The final data, however, were collected from crystals grown in polyethylene glycol (8.0 kDa) in the absence of $ZnCl_2$ after shifting pH from 7.1 to 6.7 and changing the buffer from 50 mM Tris to 50 mM cacodylate. The native as well as the Fab-peptide cocrystals were obtained by hanging drop vapor diffusion at 28ºC by using a starting Fab concentration of 10 mg/ml. A 25-fold molar excess of the peptide was used for obtaining the Fab-peptide cocrystals with minor variations of the above-described conditions.

### Data Collection

Data were collected on a MAR 300 image plate (Marresearch, Germany) installed on a rotating anode X-ray source (Rigaku, Japan) operating at 2.8 kW for the native and the Fab complexes with the peptides Slg and RII. The data for the Fab complex of the peptide Kla was collected on a MAR345dtb (Marresearch, Germany) with a rotating anode generator (Rigaku, Japan) at 5 kW. The crystals in each case were cryo-protected by soaking in mother liquor containing 25% glycerol and were flash frozen. Data were processed with DENZO (Otwinowski and Minor, 1996) and scaled with scalepack for the native dataset and for RII. Data was processed and scaled with AUTOMAR (Marresearch, Germany) for the Fab-peptide complexes of Kla and Slg.

### Structure Determination

The structure was determined by molecular replacement by using AmoRe (Navaza, 1994), and affinity-matured anti-Ars antibody 36-71 was used as the probe model in the antigen-free germline antibody. The antigen-free germline intensity data gave a good correlation coefficient ($C_F$ = 42.3%), and subsequent refinement was conducted by using this model. A progressive improvement in the correlation coefficient, $C_F$, was obtained as the structure solution for each successive antigen bound germline intensity dataset was obtained. The highest correlation coefficient ($C_F$ = 66.3%) was obtained for the Fab-peptide complex of Slg, which had similar unit cell dimensions as the probe model, the Fab-RII complex. Subsequent refinement was done starting with the corresponding models.

### Refinement

Further refinement was conducted with CNS (Brunger et al., 1998) for each of the structures. Both conventional $R_{cryst}$ and $R_{free}$ (Brunger, 1993) values (10% of total reflections in each case) were monitored during the refinement. Initially, rigid body refinement was carried out for the whole Fab molecule, and, subsequently, $V_H$, $V_L$, $C_H$, and $C_L$ domains were treated as discrete units. The model was further refined by using the positional refinement protocol of CNS. Initial attempts at utilization of NCS were abandoned due to its failure in aiding refinement. This was rationalized in terms of conformational differences arising due to flexibility in germline antibodies. Electron density maps were displayed with the help of program O (Jones et al., 1991), and the sequence of the affinity-matured antibody was slowly changed to that of the germline antibody during iterative refinement. As the refinement progressed, the peptides could be built into the electron density within the respective antigen-combining sites. Water molecules were added by using the water_pick program in CNS. The overall quality of the model was checked with PROCHECK (Laskowski et al., 1993) and WHATCHECK (Hooft et al., 1996). Final refinement statistics for the four crystal structures are given in Table 2.

### Supplemental Data

Supplemental Data including tabulations of epitope-paratope contacts, structural properties of the Fab molecules, sections of the electron density maps corresponding to the paratope as well as the epitopes, and the comparison of the independent molecules within the asymmetric units of three different structures in terms of conformational superimpositions, Cα distances, and the temperature factors of the CDRs are available at http://www.immunity.com/cgi/content/full/24/4/429/DC1/.

### Acknowledgments

We would like to thank Dr. Tim Manser for gift of the anti-Ars hybridoma, H.S. Sarna and Z. Siddiqui for technical assistance, and Drs. T.P. Singh, S. Rath, and K. Suguna for useful discussions. Financial support from the Department of Biotechnology and the Indian Council of Medical Research, Government of India is gratefully acknowledged.

Received: October 14, 2005
Revised: January 9, 2006
Accepted: February 10, 2006
Published: April 18, 2006

### References

Brunger, A.T. (1993). Assessment of phase accuracy by cross validation: the free R value. Methods and applications. Acta Crystallogr. D Biol. Crystallogr. *49*, 24–36.

Brunger, A.T., Adams, P.D., Clore, G.M., DeLano, W.L., Gros, P., and Grosse-Kunstleve, R.W. (1998). Crystallography and NMR system: A new software suite for macromolecular structure determination. Acta Crystallogr. D Biol. Crystallogr. *54*, 905–921.

Chothia, C., and Lesk, A.M. (1987). Canonical structures for the hypervariable regions of immunoglobulins. J. Mol. Biol. *196*, 901–917.

Chothia, C., Lesk, A.M., Tramontano, A., Levitt, M., Smith-Gill, S.J., Air, G., Sheriff, S., Padlan, E.A., Davies, D., and Tulip, W.R. (1989). Conformations of immunoglobulin hypervariable regions. Nature *342*, 877–883.

Cook, G.P., and Tomlinson, I.M. (1995). The human immunoglobulin VH repertoire. Immunol. Today *16*, 237–242.

Davis, M.M. (2004). The evolutionary and structural 'logic' of antigen receptor diversity. Semin. Immunol. *16*, 239–243.

Foote, J., and Milstein, C. (1994). Conformational isomerism and the diversity of antibodies. Proc. Natl. Acad. Sci. USA *91*, 10370–10374.

Garcia, K.C., Degano, M., Pease, L.R., Huang, M., Peterson, P.A., Teyton, L., and Wilson, I.A. (1998). Structural basis of plasticity in T cell receptor recognition of a self peptide-MHC antigen. Science *279*, 1166–1172.

Goel, M., Krishnan, L., Kaur, S., Kaur, K.J., and Salunke, D.M. (2004). Plasticity within the antigen-combining site may manifest as molecular mimicry in the humoral immune response. J. Immunol. *173*, 7358–7367.

Hooft, R.W.W., Vriend, G., Sander, C., and Abola, E.E. (1996). Errors in protein structures. Nature *381*, 272.

James, L.C., and Tawfik, D.S. (2003). Conformational diversity and protein evolution – a 60-year-old hypothesis revisited. Trends Biochem. Sci. *28*, 361–368.

James, L.C., Roversi, P., and Tawfik, D.S. (2003). Antibody multispecificity mediated by conformational diversity. Science *299*, 1362–1367.

Jones, T.A., Zou, J.Y., Cowan, S.W., and Kjeldgaard, M. (1991). Improved methods for building protein models in electron-density maps and the location of errors in these models. Acta Crystallogr. A *47*, 110–119.

Keitel, T., Kramer, A., Wessner, H., Scholz, C., Schneider-Mergener, J., and Hohne, W. (1997). Crystallographic analysis of anti-p24 (HIV-1) monoclonal antibody cross-reactivity and polyspecificity. Cell *91*, 811–820.

Laskowski, R.A., MacArthur, M.W., Moss, D.S., and Thornton, J.M. (1993). PROCHECK: a program to check the stereochemical quality of protein structures. J. Appl. Crystallogr. *26*, 283–291.

Manivel, V., Sahoo, N.C., Salunke, D.M., and Rao, K.V. (2000). Maturation of an antibody response is governed by modulations in flexibility of the antigen-combining site. Immunity *13*, 611–620.

Manivel, V., Bayiroglu, F., Siddiqui, Z., Salunke, D.M., and Rao, K.V.S. (2002). The primary antibody repertoire represents a linked network of degenerate antigen specificities. J. Immunol. *169*, 888–897.

Mason, D. (1998). A very high level of crossreactivity is an essential feature of the T-cell receptor. Immunol. Today *19*, 395–404.

Nair, D.T., Singh, K., Sahu, N., Rao, K.V., and Salunke, D.M. (2000). Crystal structure of an antibody bound to an immunodominant peptide epitope:novel features in peptide-antibody recognition. J. Immunol. *165*, 6949–6955.

Nair, D.T., Singh, K., Siddiqui, Z., Nayak, B.P., Rao, K.V.S., and Salunke, D.M. (2002). Epitope recognition by diverse antibodies suggests conformational convergence in an antibody response. J. Immunol. *168*, 2371–2382.

Navaza, J. (1994). AMoRe: an automated package for molecular replacement. Acta Crystallogr. A *50*, 157–163.

Nguyen, H.P., Set, N.O.L., MacKenzie, C.R., Brade, L., Kosma, P., Brade, H., and Evans, S.V. (2003). Germline antibody recognition of distinct carbohydrate epitopes. Nat. Struct. Biol. *10*, 1019–1025.

Otwinowski, Z., and Minor, W. (1996). Processing of x-ray diffraction data collected in oscillation mode. Methods Enzymol. *276*, 307–325.

Parhami-Seren, B., Kussie, P.H., Strong, R.K., and Margolies, M.N. (1993). Conservation of binding site geometry among p-azophenylarsonate- specific antibodies. J. Immunol. *150*, 1829–1837.

Ramirez-Benitez, M.C., and Almagro, J.C. (2001). Analysis of antibodies of known structure suggests a lack of correspondence between the residues in contact with the antigen and those modified by somatic hypermutation. Proteins *45*, 199–206.

Robertson, S.M., Clayton, L., Dev, V.G., Wall, R., Capra, J.D., and Kettman, J.R. (1982). Antiarsonate antibody response: a model for studying antibody diversity. Fed. Proc. *41*, 2502–2506.

Romesberg, F.E., Spiller, B., Schultz, P.G., and Stevens, R.C. (1998). Immunological origins of binding and catalysis in a Diels-Alderase antibody. Science *279*, 1929–1933.

Sharon, J., Gefter, M.L., Wysocki, L.J., and Margolies, M.N. (1989). Recurrent somatic mutations in mouse antibodies to p-azophenylarsonate increase affinity for hapten. J. Immunol. *142*, 596–601.

Sompuram, S.R., and Sharon, J. (1993). Verification of a model of a F(ab) complex with phenylarsonate by oligonucleotide-directed mutagenesis. J. Immunol. *150*, 1822–1828.

Strong, R.K., Cambell, R., Rose, D.R., Petsko, G.A., Sharon, J., and Margolies, M.N. (1991). Three dimensional Structure of Murine Anti-p-azophenylarsonate Fab 36–71. X-ray crystallography, site-directed mutagenesis, and modeling of the complex with hapten. Biochemistry *30*, 3739–3748.

Tonegawa, S. (1983). Somatic generation of antibody diversity. Nature *302*, 575–581.

Vora, K.A., Tumas-Brundage, K.M., and Manser, T. (1998). A periarteriolar lymphoid sheath-associated B cell focus response is not observed during the development of the anti-arsonate germinal center reaction. J. Immunol. *160*, 728–733.

Wang, Y., Huang, G., Wang, J., Molina, H., Chaplin, D.D., and Fu, Y.X. (2000). Antigen persistence is required for somatic mutation and affinity maturation of immunoglobulin. Eur. J. Immunol. *30*, 2226–2234.

Webster, D.M., Henry, A.H., and Rees, A.R. (1994). Antibody-antigen interactions. Curr. Opin. Struct. Biol. *4*, 123–129.

Wedemayer, G.J., Patten, P.A., Wang, L.H., Schultz, P.G., and Steven, R.C. (1997). Structural insights into the evolution of an antibody combining site. Science *276*, 1665–1669.

Wilson, I.A., and Stanfield, R.L. (1993). Antibody-antigen interactions. Curr. Opin. Struct. Biol. *3*, 113–118.

Yin, J., Mundorff, E.C., Yang, P.L., Wendt, K.U., Hanway, D., Stevens, R.C., and Schultz, P.G. (2001). A comparative analysis of the immunological evolution of antibody 28B4. Biochemistry *40*, 10764–10773.

Yin, J., Beuscher, A.E., 4th, Andryski, S.E., Stevens, R.C., and Schultz, P.G. (2003). Structural plasticity and the evolution of antibody affinity and specificity. J. Mol. Biol. *330*, 651–656.

Young, A.C., Valadon, P., Casadevall, A., Scharff, M.D., and Sacchettini, J.C. (1997). The three-dimensional structures of a polysaccharide binding antibody to Cryptococcus neoformans and its complex with a peptide from a phage display library: implications for the identification of peptide mimotopes. J. Mol. Biol. *274*, 622–634.

### Accession Numbers

Coordinates of 36-65 Fab, the 36-65 Fab-RII complex, the 36-65 Fab-KIa complex, and the 36-65 Fab-SIg complex have been deposited in the Protein Data Bank with accession codes 2A6J, 2A6D, 2A6I, and 2A6K, respectively.